The Veterinary Journal 251 (2019) 105340

Contents lists available at ScienceDirect

The Veterinary Journal

journal homepage: www.elsevier.com/locate/tvjl

A short-term evaluation of a thermoplastic polyurethane implant for osteochondral defect repair in an equine model

N.M. Korthagen[a,b], H. Brommer[a], G. Hermsen[c], S.G.M. Plomp[a], G. Melsom[c], K. Coeleveld[d], S.C. Mastbergen[d], H. Weinans[b], W. van Buul[c], P.R. van Weeren[a,*]

[a] Department of Equine Sciences, Faculty of Veterinary Medicine, Utrecht University, The Netherlands
[b] Department of Orthopaedics, Regenerative Medicine Center, University Medical Center Utrecht, Utrecht University, The Netherlands
[c] JointSphere BV, Eindhoven, The Netherlands
[d] Department of Rheumatology and Clinical Immunology, Regenerative Medicine Center, University Medical Center Utrecht, Utrecht University, The Netherlands

ARTICLE INFO

Article history:
Accepted 16 July 2019

Keywords:
Cartilage repair
Equine
Implant
Osteochondral defect
Surgical

ABSTRACT

Cartilage repair remains a major challenge and treatment of (osteo)chondral defects generally results in poor quality fibrous repair tissue. Our approach aims to address some of the major biomechanical issues encountered in scaffold-based cartilage repair, such as insufficient stiffness of the scaffolds, step formation at the interface with the native tissue and inadequate integration with the original tissue. Two osteochondral defects were created on the medial femoral trochlear ridge in each stifle of six Shetland ponies. The defects were filled with a bi-layered implant consisting of a polyetherketoneketone (PEKK) bone anchor and a polyurethane elastomer. The defects in the contralateral joint served as unfilled controls. After 12 weeks, the ponies were euthanased and tissues were evaluated macroscopically and using micro-computed tomography, histology and immunohistochemistry.

Post-operative recovery was good in all ponies and minimal lameness was observed. After 12 weeks, the proximally located plug was partially covered (mean ± standard deviation [SD] percentage surface area covered 72.5 ± 19.7%) and the distal plug was nearly completely covered (mean ± SD percentage surface area covered 98.5 ± 6.1%) with stiff and smooth repair tissue. Histology and immunohistochemistry confirmed that the repair tissue was well connected to the native cartilage but contained negligible amounts of collagen type II and glycosaminoglycans (GAGs). The repair tissue was stiff and fibrous in nature and presented a nearly flush surface with the surrounding native cartilage distally. This approach therefore resolves a number of issues related to scaffold-based cartilage repair and compares favourably with results of several other studies in large animal models. However, long-term follow-up is needed to evaluate the true potential of this type of implant.

Introduction

Traumatic articular cartilage defects are common in people (McAdams et al., 2010). They are associated with pain and reduced function and often require surgical intervention. Articular hyaline cartilage does not spontaneously regenerate, which is related to the limited anabolic synthesis of new extracellular matrix (ECM) components (Heinemeier et al., 2016). The extrinsic repair induced by bone components normally results in the formation of fibrocartilage that is biomechanically inferior compared to the original hyaline cartilage and is prone to deterioration with concomitant degeneration of the native cartilage surrounding the defect (Hunziker, 1999). Current surgical treatments include microfracture (Steadman et al., 2001), autologous chondrocyte implantation (Harris et al., 2010; Peterson et al., 2010) and osteochondral transplantation (Krych et al., 2012). However, none of these therapies result in fully satisfactory repair and all will eventually lead to the formation of biomechanically inferior fibrocartilaginous repair tissue that may contribute to the degeneration of cartilage surrounding the defect and hence, to the progression of osteoarthritis (OA). Filling the defect with a biologic or synthetic implant may offer a solution and several approaches have been developed, including those based on advanced biofabrication techniques, which often provide encouraging results when tested under in vitro conditions or experimentally in small animals (Yang et al., 2010; Benders et al., 2014; Visser

* Corresponding author.
E-mail address: r.vanweeren@uu.nl (P.R. van Weeren).

http://dx.doi.org/10.1016/j.tvjl.2019.105340
1090-0233/

et al., 2015; Zhao et al., 2016). However, few techniques and constructs have been tested in large animal models and in those studies, results were often substantially less positive than in the preceding preliminary work (Schagemann et al., 2016; Vindas Bolaños et al., 2017). Important determinants of success or failure are the mechanical properties of the implants, which in the case of artificial constructs are often substantially inferior to native tissue (Hollister, 2005), and their integration into the native bone and cartilage surrounding the defect (Bal et al., 2010; Shimomura et al., 2014). Further, it is also essential that the surface of an implant is flush with the surrounding undamaged tissue and is of comparable stiffness. The surrounding tissue of an osteochondral defect is known to deteriorate over time (Katagiri et al., 2017), which is most likely initiated by the presence of a physical 'step' due to the absence of tissue and/or the presence of a sharp transition in stiffness at the edge of the native tissue. These factors may also cause damage to opposing cartilage surfaces in the form of so-called 'kissing lesions' (Custers et al., 2007).

The purpose of this study was to test a novel type of osteochondral implant that specifically addresses the above-mentioned issues, in an equine model. The implant was bi-layered, consisting of a base made of polyetherketoneketone (PEKK) that anchors the implant to the native bone and an elastomer top layer that consists of a thermoplastic polyurethane, which has mechanical properties similar to hyaline cartilage. The elastomer was loaded with collagen-mimetic peptides 'RGD' (arginine-glycine-aspartic acid) and 'GFOGER' (glycine-phenylalanine-hydroxyproline-glycine-glutamic acid-arginine), sequence motifs containing the biofunctional domains of ECM proteins present in human hyaline cartilage, which are supposed to provide the correct biochemical cues to induce chondrocyte attachment and differentiation, thereby enhancing repair (Reyes et al., 2007). Prior to in vivo evaluation, this was examined in vitro. Positioning the implant just below the surface of the native hyaline cartilage would prevent the formation of a large 'step', whilst permitting formation of a layer of neocartilage on the elastomer. The elastomer with its mechanical properties approaching that of native cartilage and the thin (0.5 mm) layer of neo-tissue that would be formed on top of it would then result in a filling of the defect with material with appropriate stiffness.

The hypotheses were: (1) The protein-covered stiff elastomer would lead to the formation of repair tissue over the implant that would completely fill the defect and become flush with the surrounding healthy tissue within a reasonable time, thus avoiding 'step' formation; (2) The repair tissue that was expected to fill up the space above the implant would experience loading, because it would be confined in the small space between the opposing joint surface and the stiff elastomer. The loading (which in the case of the femoral trochlea will have both a compressive and a shear component) would lead to improved biomechanical properties and would enhance chondrogenic differentiation; and (3) The neo-tissue would attach to the underlying elastomer thanks to the presence of the collagen-mimetic peptides.

Materials and methods

Implant

Cylindrical implants (diameter 6.0 mm, length 7.0 mm) with a medical-grade polyetherketoneketone (PEKK) base and elastomer top layer (Fig. 1) were used in this study. The elastomer top layer consisted of a polycarbonate based aliphatic polymer containing cartilage-derived peptides 'RGD' and 'GFOGER'.

In vitro experiment

An in vitro study was performed to evaluate the behaviour of chondrocytes seeded on the elastomer surface. Equine chondrocytes were isolated under sterile conditions from macroscopically healthy stifle joints of a 7-year-old warmblood horse that was euthanased in our clinic for reasons unrelated to this study, with consent of the owner. Cartilage was digested overnight in type II collagenase (Worthington Biochemical Corporation) at 37 °C and the resulting cell suspension was filtered and washed in phosphate-buffered saline (PBS) and stored in liquid nitrogen until use. Chondrocytes were thawed and cultured for 3 to 4 weeks in Dulbecco's Modified Eagle Medium (DMEM; Life Technologies) with 2% human serum albumin (HSA; Sigma), 2% l-ascorbic acid-2-phosphate (AsAp; Sigma), 2% insulin-transferrin-selenium (ITS)-X and antibiotics (100 units/mL penicillin and 100 μg/mL streptomycin; Gibco, Life Technologies). The chondrocytes were then transferred to the elastomer and cultured in a 24-well plate on coverslips. The medium was refreshed three times per week. Chondrocytes were cultured on the coverslips for approximately 2 weeks before being stained with Alcian Blue or immunostained for collagen type II. In short, the coverslips containing the chondrocytes were fixed with 2% formaldehyde and washed three times with PBS. Alcian Blue (pH 2.5) was added for 15 min, the coverslips were washed with PBS and counterstained with Nuclear fast red for 5 min. After counterstaining, the coverslips were washed very briefly (<1 min) with tap water and mounted on slides using Xylene/Depex. For collagen type II staining, the cells were blocked with 5% normal goat serum (NGS) for 30 min and then incubated with mouse monoclonal antibody (DSHB, II-IIB63, diluted 1:100 in 2% NGS) overnight. The next day the coverslips were washed with PBS and incubated with goat anti-mouse IgG-peroxidase conjugated (DAKO, P0447 1:100 in 2% NGS). After washing with PBS, the slides were incubated in 3,3′-diaminobenzidine (DAB) substrate (Vector Laboratories) for 5 min and then counterstained with Mayer's haematoxylin solution. After rinsing with tap water for 10 min, the slides were mounted using xylene/Depex.

Experimental animals and procedure

A preparatory species-specific safety (biocompatibility) study was performed in one 6-year old male Shetland pony (body mass 156 kg). The subsequent osteochondral implant study was performed in six Shetland ponies (5 mares and one gelding), mean ± standard deviation (SD) age 7.3 ± 3.2 years (range 3–12 years), mean ± SD body mass 150 ± 16 kg. Animals were housed in individual box stalls with solid walls that allowed visual contact and could acclimatise for at least a week prior to the start of the experiment.

For the subcutaneous safety study, the pony received premedication with detomidine (10 mg kg IV) and morphine (0.2 mg kg IV). One mL local anaesthetic solution (mepivacaine 2%) was injected subcutaneously before incision and the incision sites were closed in routine fashion using two to three simple interrupted sutures of Ethilon nylon size 0 (Ethicon). Post-operatively, the pony was monitored twice daily for general health, temperature and feeding status, and at least once a day for experiment-specific effects such as heat, swelling or infection of the implant

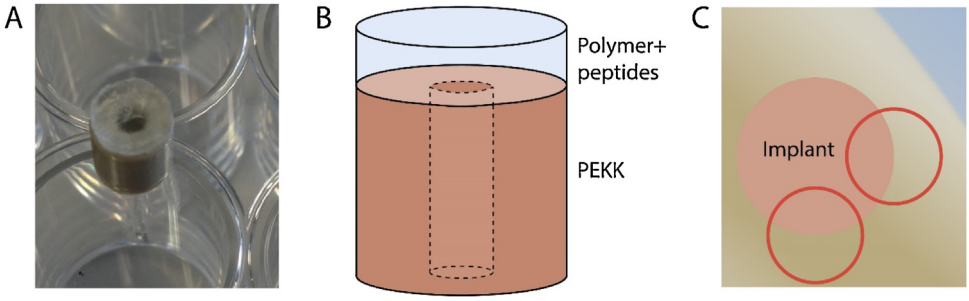

Fig. 1. (A) Picture of the implant consisting of a polyetherketoneketone (PEKK) base and a transparent elastomer top consisting of polycarbonate loaded with collagen-mimetic peptides 'RGD' (arginine-glycine-aspartic acid) and 'GFOGER' (glycine-phenylalanine-hydroxyproline-glycine-glutamic acid-arginine). (B) Schematic representation of the implant. (C) Biopsy locations shown in red.

area. Additional analgesia was available in case of adverse events, but was not administered as the pony did not show signs of pain on examination. Humane endpoints were determined a priori based on general health examinations and were approved by the local animal welfare committee; these endpoints were not reached.

Different components of the implant, with and without cartilage-derived peptides, were implanted subcutaneously in the neck region of the pony. Titanium and commercially available fibrin glue of human origin (TISSEEL, Baxter International) were included as controls and each material was randomly allocated to a surgically created pocket at least 5 cm from the other implantation sites; stratified randomisation using randomisation software was used to ensure that materials containing peptides were not immediately adjacent to each other). After 19 days, the animal was euthanased and the materials were explanted with the surrounding tissue and processed for paraffin histology.

For the osteochondral defect model, the six ponies were first evaluated for lameness using the American Association of Equine Practitioners (AAEP) grading scale (0–5) and were all clinically sound (grade 0). After premedication with detomidine (10 mg/kg IV) and morphine (0.2 mg/kg IV) and placement of a 16G jugular venous catheter, ponies received peri-operative antibiotic prophylaxis (ampicillin 15 mg/kg IV and procaine penicillin 20 mg/kg IM) and non-steroidal anti-inflammatory medication (meloxicam 0.6 mg/kg IV). Anaesthesia was induced with diazepam (0.06 mg/kg IV) and ketamine (2.2 mg/kg IV) and maintained with isoflurane in oxygen (fraction of inspired oxygen 60–90%), supplemented with a constant rate infusion of ketamine (0.5 mg/kg/h) and detomidine (10 μg/kg/h) for inhalant-sparing and analgesic effects. Post-operatively (PO), the ponies received meloxicam (0.6 mg/kg orally twice daily on day 1, and once daily from day 2 onwards) and tramadol (5 mg/kg PO twice daily) for 5 days. Ponies were closely monitored with a twice-daily general examination as well as objective pain assessment (every 4 h for the first 48 h) using EQUUS-COMPASS (Van Loon and Van Dierendonck, 2015) and daily lameness assessment. Cut-off for rescue analgesia was determined a priori at a composite pain score >9 or >3/5 lameness (on the AAEP scale). No adjunctive epidural analgesia was required in any of the ponies during the study. Severe lameness due to joint infection was considered a humane end-point that would result in immediate euthanasia; no cases of infectious arthritis occurred.

Osteochondral defects were surgically induced in two sites on the medial trochlear ridge of the femur (one located proximally and one more distally) in both femoropatellar joints, following an earlier described procedure (Vindas Bolaños et al., 2017). In short, a 5–6 cm incision was made between the medial and middle patellar ligament, through the skin, subcutaneous tissues, fascia and joint capsule. An orthopaedic drill with a 5.9 mm diameter bit and the corresponding drill guide were used to create lesions of 5.9 mm diameter and 7.5 mm depth. Implants (diameter 6.0 mm, length 7.0 mm) were press fit into place 0.5 mm under the cartilage surface in both defects, in either the left or right stifle joint (decided by simple randomisation using a coin toss). In the contralateral joint, similar defects were created, which were left untreated to serve as controls. The joint capsule and the fascia were closed with simple interrupted sutures (Vicryl size 0, Ethicon). The subcutis and the skin were closed in a continuous suture pattern with Vicryl size 2/0 and Ethilon nylon size 0 (Ethicon), respectively. After the surgery, ponies were box-rested for 3 weeks, hand-walked for 1 week and then turned out in a large field. Box stalls contained woodchip bedding and hay and water was provided ad libitum. Arthroscopic re-revaluation was performed after 3 weeks in one pony, as a go/no-go check prior to performing the surgery on the five remaining ponies.

At the end of the study, after 12 weeks, the ponies were euthanased and the hind limbs were disarticulated at the coxofemoral joints. The femoropatellar joints were opened and the overall condition of the joint, the colour of the repair tissue, and the attachment of any repair tissue to surrounding bone and cartilage and to the underlying elastomer were assessed. All defects were manually probed with a standard arthroscopic hook probe and photographed.

This research was approved by the Dutch Central Animal Experiments Committee (Approval number AVD108002015307; these specific animal experiments were approved on 25 May 2016 by the local animal welfare committee).

Tissue collection and processing

Biopsies (4 mm diameter) were taken on the edge of the defect area so that they contained both full thickness native cartilage tissue and repair tissue (Fig. 1) and were fixed in 4% formaldehyde solution (Klinipath). After serial dehydration in graded ethanol solutions and xylene (Brunschwig Chemie), they were embedded in paraffin and evaluated using histology and immunohistochemistry.

The remaining implant with at least 1 cm surrounding tissue was dissected using an electric oscillating saw, fixed in formaldehyde and a micro-computed tomography scan (3 min scan time, 42 μm voxel size, 90 kV tube voltage, 180 μA tube current) was performed (Quantum FX, Perkin Elmer). Subsequently, the formalin fixed samples were embedded in polymethylmethacrylate (PMMA).

Histology and immunohistochemistry

Coronal sections with a thickness of 5 μm were cut from the biopsies and deparaffinised and stained with haematoxylin and eosin (H and E), Safranin O/fast green (SafO), and immune stained for collagen I and collagen II.

For H and E, sections were stained with Mayer's haematoxylin solution (Merck), rinsed and then stained with 0.2% Eosin Y solution (Merck). SafO sections were first stained with Weigert's Haematoxylin solution (Klinipath), then with 0.4% aqueous

Table 1
Osteoarthritis Research Society International (OARSI) histocompatibility score for horses as described in McIlwraith et al. (2010).

Outcome parameter	Score	Description
Chondrocyte necrosis	0	Normal section without necrosis
	1	No more than one necrotic cell located near the articular surface per 20× objective
	2	One or two necrotic cells located near the articular surface per 20× objective
	3	Two or three necrotic cells located near the articular surface per 20× objective
	4	Three or four necrotic cells located near the articular surface per 20× objective
Cluster (complex chondrone) formation	0	No cluster formation throughout section
	1	Two chondrocytes (doublets) within same lacunae along superficial aspect of the articular cartilage section
	2	Two or three chondrocytes (doublets and triplets) within same lacunae along superficial aspect of the articular cartilage section
	3	Three or four chondrocytes within same lacunae along superficial aspect of the articular cartilage section
	4	Greater than four chondrocytes within same lacunae along superficial aspect of the articular cartilage section
Fibrillation/fissuring	0	No fibrillation/fissuring of the articular cartilage surface
	1	Fibrillation/fissuring of the articular cartilage restricted to surface and superficial zone
	2	Fissuring that extends into the middle zone
	3	Fissuring that extends to the level of the deep zone
	4	Fissuring that extends into the deep zone
Focal cell loss	0	Normal cell population throughout the section
	1	A 10–20% area of acellularity per 20× field
	2	A 20–30% area of acellularity per 20× field
	3	A 40–50% area of acellularity per 20× field
	4	A greater than 50% area of acellularity per 20× field
Safranin O Fast Green stain uptake	0	Normal staining
	1	Less than 25% loss of staining characteristics
	2	25–50% loss of staining characteristics
	3	50–75% loss of staining characteristics
	4	Greater than 75% loss of staining characteristics

Fast Green (Sigma–Aldrich), subsquently rinsed twice in 1% Acetic Acid, and finally stained with 0.125% Aqueous Safranin-O (Sigma–Aldrich).

For collagen I and II, sections were first blocked with 0.3% H_2O_2. As antigen retrieval, sections were successively treated with 1 mg/mL pronase from Streptomyces griseus (Roche) and then with 10 mg/mL hyaluronidase (Sigma–Aldrich) for 20–30 min at 37 °C. Collagen I primary antibody was rabbit monoclonal ab138492 (Abcam) and as secondary antibody EnVision + System-HRP Anti-Rabbit (K4003, DAKO) was used. Normal Rabbit IgG (X0903, DAKO) was used as the negative control. Collagen II primary antibody was mouse monoclonal Col2A1 Antibody II-II6B3 (DSHB). As secondary antibody EnVision + System-HRP Anti-Mouse (K4001, DAKO) was used, and as a negative control normal mouse IgG1 (Santa Cruz). Finally, sections were stained with DAB peroxidase substrate solution (DAKO).

The PMMA embedded plug was cut with a Leica 4 SP1600 Saw Microtome system (Leica) to yield 50–60 μm sections and these were stained with basic fuchsine-methylene blue.

All slides were evaluated and the native cartilage directly adjacent to the defect was assessed using the Osteoarthritis Research Society International (OARSI) score for histological assessment in the horse (McIlwraith et al., 2010; Table 1). Images were obtained using an Olympus BX51 microscope and scored by two independent observers. Total scores per sample for each observer were averaged. Weighted Kappa correlation coefficients were calculated using R Project for Statistical Computing. Shapiro–Wilk normality test was performed for each group and differences were evaluated using a Kruskal–Wallis test with Dunn's multiple comparisons test using GraphPad Prism 7.04.

Results

In vitro and in vivo safety study

The cells were able to maintain their chondrocytic phenotype, as shown by the synthesis of cartilage-specific proteins: GAGs and collagen type II (Fig. 2A, B). The in vivo safety test showed that the subcutaneously implanted materials were well tolerated. Besides mild swelling at the implant site, no local or systemic clinical signs were observed. Histologically, minor cell infiltration was seen (Fig. 2C). Compared to the negative control (titanium; Fig. 2D), there was slightly more cell infiltration, mostly of eosinophils. However, infiltration was minimal compared to xenogeneic fibrin glue (Fig. 2E).

Clinical evaluation

Post-operative recovery was good in all ponies. One day post-operatively, clinical evaluation revealed decreased range of motion of both hind limbs in all ponies, but no abnormalities in limb-loading. On the second day post-surgery, the stiffness was resolved, and no lameness was observed during the rest of the study period. All surgical wounds healed uneventfully, without any signs of infection.

Arthroscopic and macroscopic evaluations

Arthroscopic re-evaluation at 3 weeks in one pony, and post mortem macroscopic evaluation at 12 weeks in all animals ($n = 6$) showed partial covering of the proximal plug (complete surface coverage in 2/6 ponies; mean ± standard deviation [SD] percentage surface covering 72.5 ± 19.7%) and complete covering in 5/6 ponies of the distal plug (mean ± SD percentage surface covering 97.5 ± 6.1%) with a smooth repair tissue, flush with the surrounding surface (Figs. 3 and 4 A). The repair tissue formed on the implant could not be compressed with the hook probe but could be lifted from the surface of the implant. The tissue filling the defect and covering the elastomer was well attached to the native cartilage but was not attached to any of the implants.

No macroscopic abnormalities were observed in the surrounding soft tissues and no kissing lesions were observed on the opposing articular surface of the patella in either group. The control defects typically showed incomplete filling of the defect with very soft fibrous repair tissue that could easily be deformed with the hook probe.

Evaluation by micro-computed tomography

Micro-computed tomography analysis (Fig. 4B) showed only minor irregularities in the bone surrounding the implant. In the untreated defect, irregular bone formation occcured and abnormalities were present in the underlying pre-existing bone.

Histology and immunohistochemistry

The repair tissue was well attached to the native cartilage but there was a clearly visible transition between the tissues. Where the native cartilage was positive for collagen II and GAGs on SafO staining, both at the proximal and distal location, the repair tissue

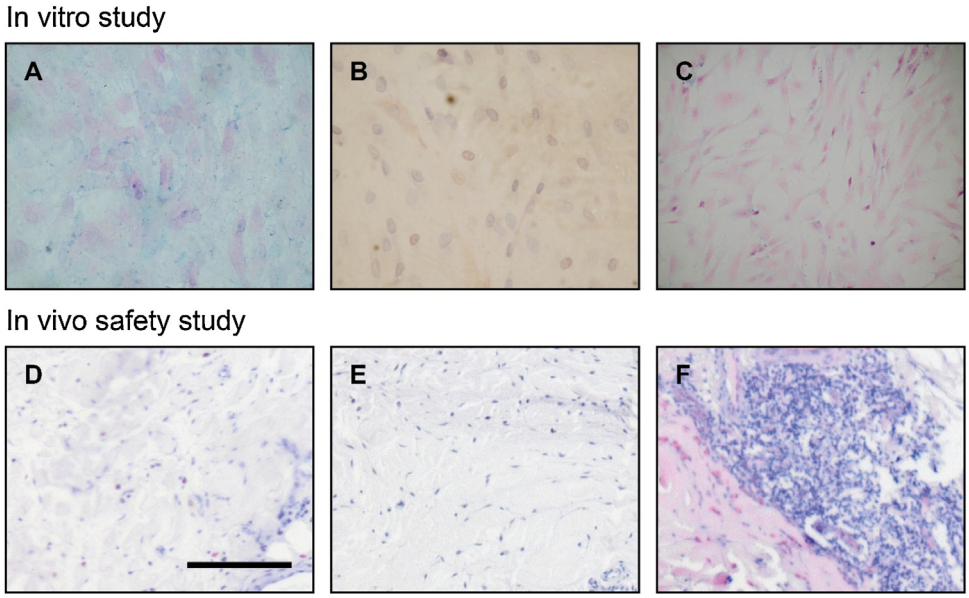

Fig. 2. (A, B, C): In vitro study. Chondrocytes cultured on the elastomer stained with Alcian Blue (A) and with immunostaining for collagen type II in brown (B); negative control (C). (D, E, F): Safety study. Haematoxylin and eosin (H and E) staining of tissue adjacent to the elastomer (C); titanium implant as negative control (D); xenogeneic fibrin glue as a positive control (E). Bar indicates 200 μm.

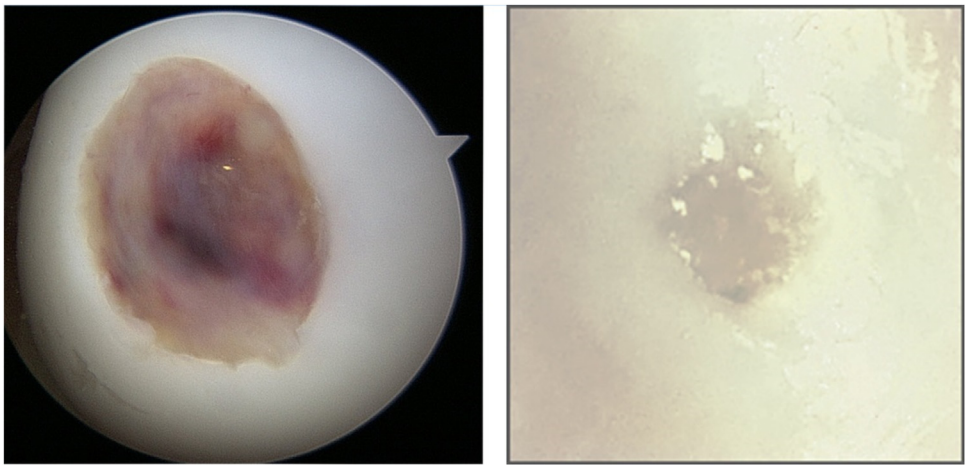

Fig. 3. (A) distal defect at week 3 as seen during arthroscopic evaluation (left) and at week 12, post mortem (right).

was positive for GAGs at a very limited number of small sites only and stained extensively positive for collagen I (Fig. 5). There were no significant differences in staining of the repair tissue between treated and untreated defects. Mild degeneration in the form of GAG loss and formation of chondron clusters was visible in the native cartilage, but only in the area directly adjacent to the defect. Assesment of degeneration using the OARSI scoring system for horses showed a median score of 6 for the distal defects for both implants and controls (scale 0–20) and a score of 7 for the proximal implant and 6 for the proximal control groups (overall 95% confidence interval (CI) [5.7–6.8]). There were no statistically significant differences between groups (Fig. 6). The weighted Kappa correlation coefficient between observers was $\kappa = 0.83$. PMMA-embedded slices of the whole defect also showed repair tissue that was well connected to the native cartilage and confirmed minimal bone abnormalities in the treated defects (Fig. 4C). Unfortunately, the elastomer was not visible in these slides and the PMMA embedding process affected the global morphology of the repair tissue, making it difficult to assess.

Discussion

Osteochondral repair continues to be a challenge in both humans and animals, especially in large animals such as the horse. Common issues include insufficient stiffness of the scaffolds, step formation at the interface with the native tissue and inadequate integration with the surrounding tissue. This study aimed to address these issues by using a novel bi-layered implant, containing collagen-mimetic peptides on the top elastomer layer, which has a relatively high stiffness. This implant was positioned just below the cartilage surface in relatively small osteochondral defects (6 mm diameter) in the stifle joints of six Shetland ponies. The implants were well tolerated and no lameness was observed during the 12-week study period. There were no macroscopic abnormalities in the surrounding tissues or on the opposing articular surface of the patella. Fixation can be another issue with both chondral and osteochondral implants, often requiring glue or sutures that can affect the surrounding native tissue (Mancini et al., 2017). No problems were encountered in this study. The implants were easy to handle and could be placed by press-fit fixation.

Our first hypothesis was that because of the small defect size and the placement of the stiff implant just below the cartilage surface, the defects would become filled with repair tissue, flush with the surrounding tissue. This was indeed observed in the distal defects, while in the more proximally located defects, repair was more partial. As the exact amount of loading at both sites and the relative contribution of shear and compressive loading are unknown, no conclusion can be drawn about our second hypothesis. The differences in filling of the proximal and distal defects, and the likelihood that loading conditions at these sites will be different, suggest an influence of loading on defect filling. There was good integration between the repair tissue and the native cartilage, but no hyaline cartilage was formed in any of the defects. Also, the repair tissue did not adhere to the elastomer, refuting our third hypothesis. This is a serious issue that may be related to the non-porous surface characteristics of the elastomer, as no ingrowth of cells was observed. Adaptation of the surface towards a more porous nature might resolve this problem. There was some mild degeneration of the native cartilage, but only directly adjacent to the defect. This degeneration was mainly characterised by complex chondron formation and loss of GAGs.

Evaluation using the OARSI score for horses showed no significant differences between treated and untreated osteochondral defects. However, the untreated osteochondral defects showed clear incomplete, concave filling. While it has previously been suggested that the critical defect size in the equine stifle is 9 mm (Convery et al., 1972; McIlwraith et al., 2011), this study clearly showed that 6-mm defects in the medial trochlear ridge are not fully repaired within 12 weeks.

Although performed only in one pony, arthroscopic comparison of the repair tissue at 3 weeks and at 12 weeks clearly showed improved structure, more complete filling and reduced redness. Virtually no hyaline cartilage formation was visible at 12 weeks, but it is conceivable that the (bio-)mechanical cues provided by the implant would induce chondrocyte differentiation and the formation of hyaline cartilage at a later stage than 12 weeks. In other large animal models (Jackson et al., 2001; Miller et al., 2014; Vindas Bolaños et al., 2017), it has been shown that defects which are incompletely filled at short-term (4–12 weeks), will inevitably lead to severe degeneration of the surrounding cartilage and bone at longer follow-up (12–52 weeks). This is therefore an issue requiring further attention when designing an implant.

The equine model was selected because of similarity to humans in terms of joint size, cartilage thickness and healing properties (Malda et al., 2012). Additionally, horses suffer from similar articular disorders as men (Van Weeren et al., 2016). The use of ponies has benefits over the use of horses because the joint size is even closer to that of humans and they are easier to house and they seem to recover faster from surgery. Unfortunately, horses present a high risk of problems related to recovery and wound healing (McIlwraith et al., 2011; Husby et al., 2016). This is partially caused by the immediate loading after surgery. The resulting compression

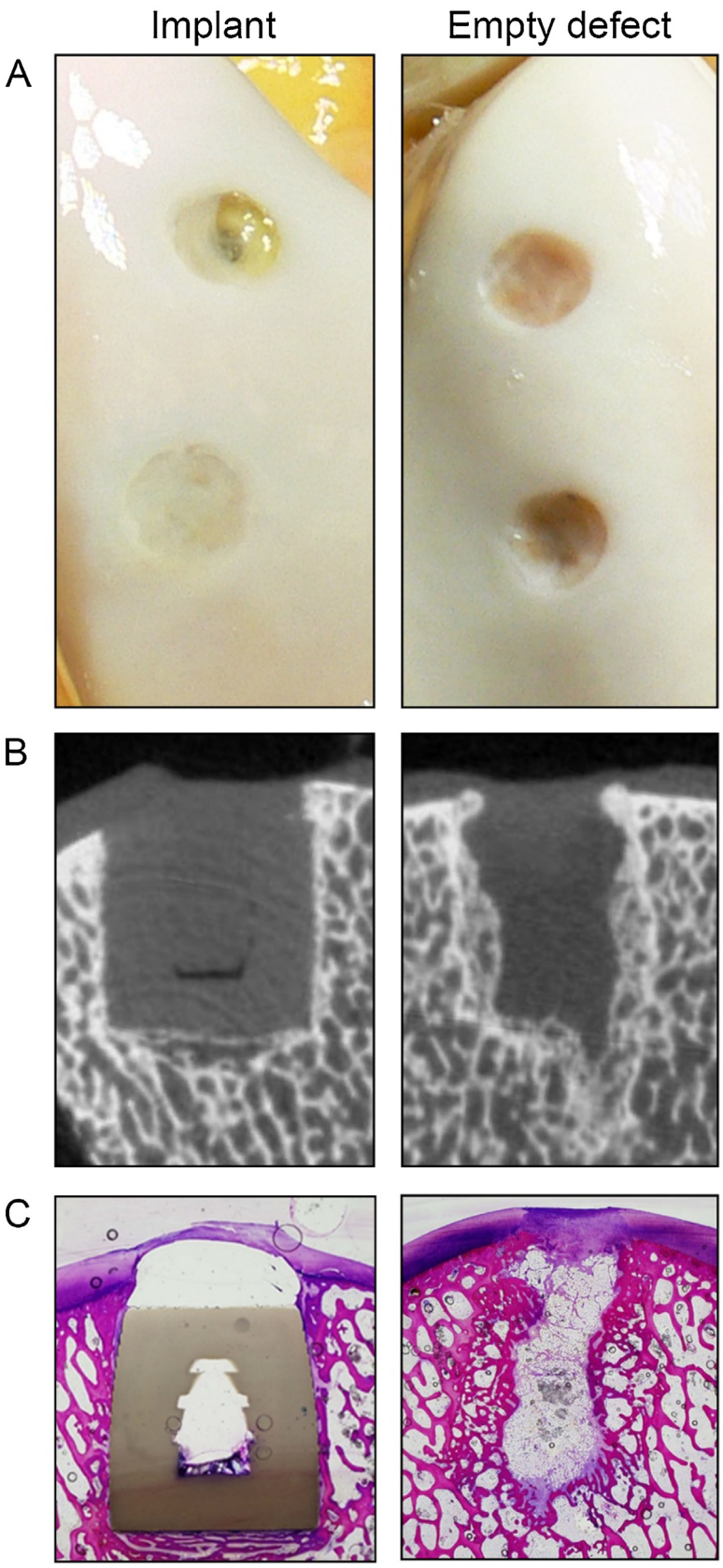

Fig. 4. Representative images of macroscopic appearance (A), micro-computed tomography scan (B) and polymethylmethacrylate (PMMA) embedded slides (C) of the defects at 12 weeks with implant (left column) or untreated control defects (right column). The polymer is not visible in the PMMA embedded slides.

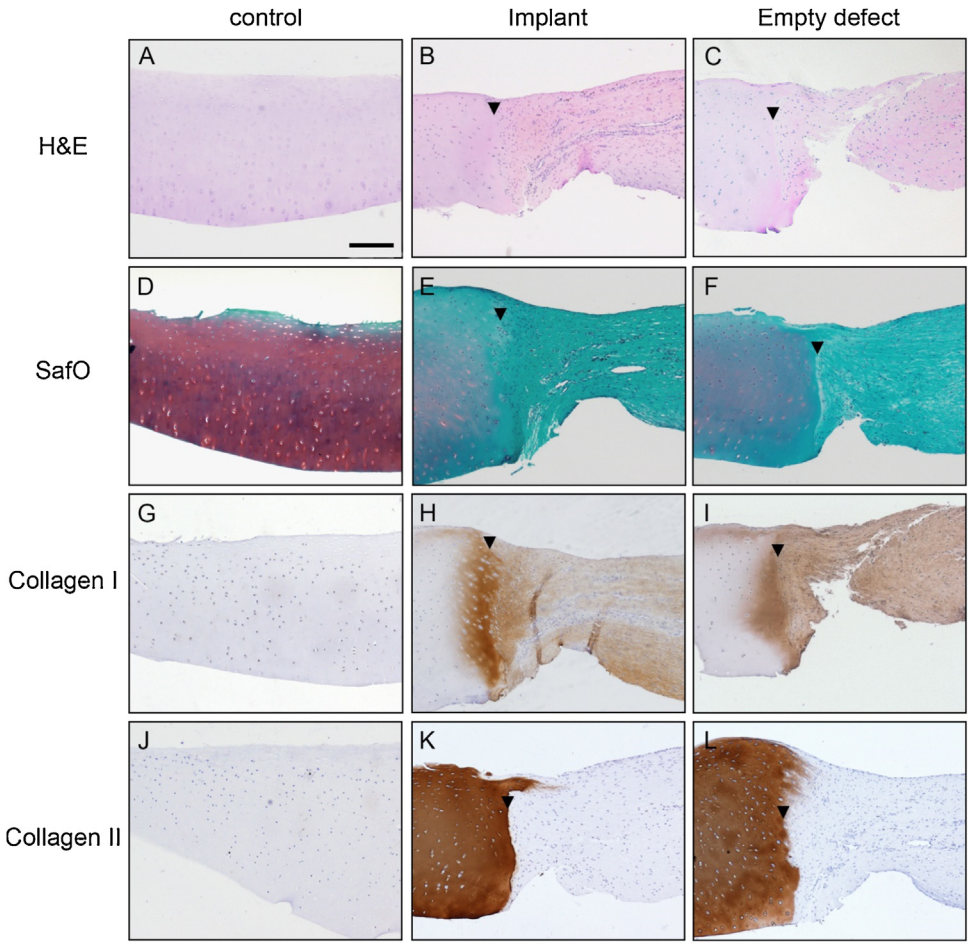

Fig. 5. Representative histochemistry slides of paraffin embedded biopsies taken across the edge of the defect (arrowhead). The original tissue is to the left in the image. 40× magnification. Bar indicates 200 μm. Positive controls for haematoxylin and eosin (H and E), Safranin O/fast green (SafO) stainings are shown (A and D, respectively). Negative (isotype) controls for collagen I and II stainings are shown (G and J, respectively).

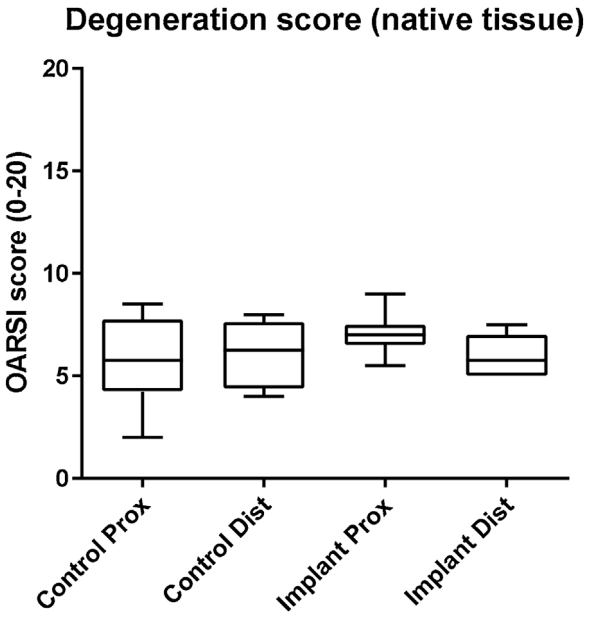

Fig. 6. Osteoarthritis Research Society International (OARSI) score of the native tissue surrounding the defect, revealing no significant differences between any of the groups.

and shear stresses may have prevented the initial formation of repair tissue and most likely resulted in the incomplete filling of the proximal defects. On the other hand, loading of chondrogenic repair tissue may aid in stimulating the formation of ECM components, especially of GAGs (Palmer et al., 1995). In combination with the mechanical properties of the currently used implant, closely mimicking the mechanical properties of healthy cartilage, the application of an exercise regimen might ensure that the right biomechanical cues are provided to optimise the quality of the repair tissue. Therefore, a long-term follow-up study including a controlled exercise regimen would be a logical next step to evaluate the potential of this implant for clinical use.

Conclusions

The implants were well tolerated and induced very minor deterioration of the surrounding native cartilage and bone. This was similar to the controls after the short study period, but the stiffness of the repair tissue covering the implants, which was flush with the surrounding tissue and well connected to it, made it likely that the native tissue surrounding the treated defects would be less prone to deterioration than that surrounding the open defects. However, the covering tissue was not connected to the elastomer and was fibrous in nature. A long-term study with improved cartilage binding properties of the elastomer, including an exercise regimen, is needed to further evaluate its potential for clinical use.

Conflict of interest statement

This study was partially funded by the Dutch Arthritis Society (grant LLP-22). This funding agency had no influence on any part of the study or the decision to submit the article for publication. Gied Hermsen, Giles Melsom and Ward van Buul have a financial relationship with Jointsphere BV who covered the material costs of the study but had no influence on the interpretation of the results. None of the other authors of this paper has a financial or personal relationship with other people or organisations that could inappropriately influence or bias the content of the paper.

References

Bal, B.S., Rahaman, M.N., Jayabalan, P., Kuroki, K., Cockrell, M.K., Yao, J.Q., Cook, J.L., 2010. In vivo outcomes of tissue-engineered osteochondral grafts. Journal of Biomedical Materials Research Part B, Applied Biomaterials 93, 164–174.

Benders, K.E., Boot, W., Cokelaere, S.M., Van Weeren, P.R., Gawlitta, D., Bergman, H.J., Saris, D.B., Dhert, W.J., Malda, J., 2014. Multipotent stromal cells outperform chondrocytes on cartilage-derived matrix scaffolds. Cartilage 5, 221–230.

Convery, F.R., Akeson, W.H., Keown, G.H., 1972. The repair of large osteochondral defects. An experimental study in horses. Clinical Orthopaedics and Related Research 82, 253–262.

Custers, R.J., Dhert, W.J., van Rijen, M.H., Verbout, A.J., Creemers, L.B., Saris, D.B., 2007. Articular damage caused by metal plugs in a rabbit model for treatment of localized cartilage defects. Osteoarthritis and Cartilage 15, 937–945.

Harris, J.D., Siston, R.A., Pan, X., Flanigan, D.C., 2010. Autologous chondrocyte implantation: a systematic review. The Journal of Bone and Joint Surgery, American Volume 92, 2220–2233.

Heinemeier, K.M., Schjerling, P., Heinemeier, J., Moller, M.B., Krogsgaard, M.R., Grum-Schwensen, T., Petersen, M.M., Kjaer, M., 2016. Radiocarbon dating reveals minimal collagen turnover in both healthy and osteoarthritic human cartilage. Science Translational Medicine 8, 346ra90.

Hollister, S.J., 2005. Porous scaffold design for tissue engineering. Nature Materials 4, 518–524.

Hunziker, E.B., 1999. Articular cartilage repair: are the intrinsic biological constraints undermining this process insuperable? Osteoarthritis and Cartilage 7, 15–28.

Husby, K.A., Reed, S.K., Wilson, D.A., Kuroki, K., Middleton, J.R., Hoepp, N.C., Charles, E.M., Cook, J.L., 2016. Evaluation of a permanent synthetic osteochondral implant in the equine medial femoral condyle. Veterinary Surgery 45, 364–373.

Jackson, D.W., Lalor, P.A., Aberman, H.M., Simon, T.M., 2001. Spontaneous repair of full-thickness defects of articular cartilage in a goat model. A preliminary study. The Journal of Bone and Joint Surgery, American Volume 83A, 53–64.

Katagiri, H., Mendes, L.F., Luyten, F.P., 2017. Definition of a critical size osteochondral knee defect and its negative effect on the surrounding articular cartilage in the rat. Osteoarthritis and Cartilage 25, 1531–1540.

Krych, A.J., Robertson, C.M., Williams 3rd, R.J., Cartilage Study Group, 2012. Return to athletic activity after osteochondral allograft transplantation in the knee. The American Journal of Sports Medicine 40, 1053–1059.

Malda, J., Benders, K.E., Klein, T.J., de Grauw, J.C., Kik, M.J., Hutmacher, D.W., Saris, D. B., van Weeren, P.R., Dhert, W.J., 2012. Comparative study of depth-dependent characteristics of equine and human osteochondral tissue from the medial and lateral femoral condyles. Osteoarthritis and Cartilage 20, 1147–1151.

Mancini, I.A.D., Vindas Bolanos, R.A., Brommer, H., Castilho, M., Ribeiro, A., van Loon, J.P.A.M., Mensinga, A., van Rijen, M.H.P., Malda, J., van Weeren, R., 2017. Fixation of hydrogel constructs for cartilage repair in the equine model: a challenging issue. Tissue Engineering Part C: Methods 23, 804–814.

McAdams, T.R., Mithoefer, K., Scopp, J.M., Mandelbaum, B.R., 2010. Articular cartilage injury in athletes. Cartilage 1, 165–179.

McIlwraith, C.W., Fortier, L.A., Frisbie, D.D., Nixon, A.J., 2011. Equine models of articular cartilage repair. Cartilage 2, 317–326.

McIlwraith, C.W., Frisbie, D.D., Kawcak, C.E., Fuller, C.J., Hurtig, M., Cruz, A., 2010. The OARSI histopathology initiative - Recommendations for histological assessments of osteoarthritis in the horse. Osteoarthritis and Cartilage 18 (Suppl. 3), S93–105.

Miller, R.E., Grodzinsky, A.J., Barrett, M.F., Hung, H.H., Frank, E.H., Werpy, N.M., McIlwraith, C.W., Frisbie, D.D., 2014. Effects of the combination of microfracture and self-assembling peptide filling on the repair of a clinically relevant trochlear defect in an equine model. The Journal of Bone and Joint Surgery, American Volume 96, 1601–1609.

Palmer, J.L., Bertone, A.L., Mansour, J., Carter, B.G., Malemud, C.J., 1995. Biomechanical properties of third carpal articular cartilage in exercised and nonexercised horses. Journal of Orthopedic Research 13, 854–860.

Peterson, L., Vasiliadis, H.S., Brittberg, M., Lindahl, A., 2010. Autologous chondrocyte implantation: A long-term follow-up. The American Journal of Sports Medicine 38, 1117–1124.

Reyes, C.D., Petrie, T.A., Burns, K.L., Schwartz, Z., Garcia, A.J., 2007. Biomolecular surface coating to enhance orthopaedic tissue healing and integration. Biomaterials 28, 3228–3235.

Schagemann, J.C., Rudert, N., Taylor, M.E., Sim, S., Quenneville, E., Garon, M., Klinger, M., Buschmann, M.D., Mittelstaedt, H., 2016. Bilayer implants: electromechanical assessment of regenerated articular cartilage in a sheep model. Cartilage 7, 346–360.

Shimomura, K., Moriguchi, Y., Ando, W., Nansai, R., Fujie, H., Hart, D.A., Gobbi, A., Kita, K., Horibe, S., Shino, K., et al., 2014. Osteochondral repair using a scaffold-free tissue-engineered construct derived from synovial mesenchymal stem cells and a hydroxyapatite-based artificial bone. Tissue Engineering Part A 20, 2291–2304.

Steadman, J.R., Rodkey, W.G., Rodrigo, J.J., 2001. Microfracture: Surgical technique and rehabilitation to treat chondral defects. Clinical Orthopaedics and Related Research (Suppl. 391), 362–369.

Van Loon, J.P., Van Dierendonck, M.C., 2015. Monitoring acute equine visceral pain with the Equine Utrecht University Scale for Composite Pain Assessment (EQUUS-COMPASS) and the Equine Utrecht University Scale for Facial Assessment of Pain (EQUUS-FAP): A scale-construction study. The Veterinary Journal 206, 356–364.

van Weeren, P.R., Back, W., 2016. Musculoskeletal disease in aged horses and its management. Veterinary Clinics of North America: Equine Practice 32, 229–247.

Vindas Bolaños, R.A., Cokelaere, S.M., Estrada McDermott, J.M., Benders, K.E., Gbureck, U., Plomp, S.G., Weinans, H., Groll, J., van Weeren, P.R., Malda, J., 2017. The use of a cartilage decellularized matrix scaffold for the repair of osteochondral defects: the importance of long-term studies in a large animal model. Osteoarthritis and Cartilage 25, 413–420.

Visser, J., Levett, P.A., te Moller, N.C., Besems, J., Boere, K.W., van Rijen, M.H., de Grauw, J.C., Dhert, W.J., van Weeren, P.R., Malda, J., 2015. Crosslinkable hydrogels derived from cartilage, meniscus, and tendon tissue. Tissue Engineering Part A 21, 1195–1206.

Yang, Z., Shi, Y., Wei, X., He, J., Yang, S., Dickson, G., Tang, J., Xiang, J., Song, C., Li, G., 2010. Fabrication and repair of cartilage defects with a novel acellular cartilage matrix scaffold. Tissue Engineering Part C: Methods 16, 865–876.

Zhao, X., Papadopoulos, A., Ibusuki, S., Bichara, D.A., Saris, D.B., Malda, J., Anseth, K.S., Gill, T.J., Randolph, M.A., 2016. Articular cartilage generation applying PEG-LA-DM/PEGDM copolymer hydrogels. BMC Musculoskeletal Disorders 17, 245-016-1100-1.